ChemComm

Wavelength Dependent Photochemical Charge Transfer at the Cu_2O – $BiVO_4$ Particle Interface – Evidence for Tandem Excitation

Journal:	*ChemComm*
Manuscript ID	CC-COM-05-2018-004123.R1
Article Type:	Communication

Please do not adjust margins

Journal Name

COMMUNICATION

Wavelength Dependent Photochemical Charge Transfer at the Cu_2O – $BiVO_4$ Particle Interface – Evidence for Tandem Excitation

Zongkai Wu, Ghunbong Cheung, Jiarui Wang , Zeqiong Zhao, and Frank E. Osterloh*

Received 00th January 20xx,
Accepted 00th January 20xx

DOI: 10.1039/x0xx00000x

www.rsc.org/

The understanding of the photochemical charge transfer properties of powdered semiconductors is of relevance to artificial photosynthesis and the production of solar fuels. Here we use surface photovoltage spectroscopy to probe photoelectrochemical charge transfer between bismuth vanadate ($BiVO_4$) and cuprous oxide (Cu_2O) particles as a function of wavelength and film thickness. Optimized conditions produce a -2.10 V photovoltage under 2.5 eV (0.1 mW cm^{-2}) illumination, which suggests the possibility of a water splitting system based on a $BiVO_4$ – Cu_2O direct contact particle tandem.

The photoelectrochemical water splitting reaction can provide hydrogen fuel from only solar energy and water. To generate the required water electrolysis potential of approximately 1.6 V, two or more mid gap semiconductors are typically used in series. [1, 2] The ideal limiting solar to hydrogen efficiency of a dual absorber configuration (28 %) [3-5] is about twice that of a single absorber system. [2-9] Tandem devices for the water splitting reaction often rely on monolithic absorber stacks [10-19] that are difficult and expensive to fabricate because they require slow vacuum deposition methods, such as metal organic chemical vapour deposition (MOCVD). This problem is avoided in particle based tandem systems, where the Ohmic contact between the light absorbers is established through soluble redox couples, I_3^- /I^-, or Fe^{3+}/Fe^{2+}, or through direct physical contact. Examples for this type of tandem system include suspended TiO_2 particles, [20] tandems made of $SrTiO_3$:Ru-$BiVO_4$, [21, 22] the ZrO_2/TaON and WO_3 tandem system, [23, 24] and the RuO_2-TaON and Pt-TaON overall water splitting system. [25-27] While particle contacts are easy to manufacture, photochemical charge transfer dynamics at these 'rough' interfaces and their dependence on surface morphology, electrolyte environment, [28] and particle size are not well understood. As particles get smaller, the effect of internal electric fields (space charge layers) diminishes, and charge transfer is dominated by the relative concentrations of the charge carriers, the energetics of donor and acceptor configuration, and by surface and interfacial states of the particles. [29] Understanding these factors is important for raising the energy conversion efficiency of particle-based systems. Here we use surface photovoltage spectroscopy (SPS) to study photochemical charge transfer at the interfaces of Cu_2O and $BiVO_4$ nanoparticles. In SPS, the contact potential difference (CPD) of a sample film is measured under illumination with a semi-transparent Kelvin probe. [30-33] A photovoltage (ΔCPD) can result from the movement of the charge carriers through the film or from their transfer across the interface between the particle film with another component of the circuit.[34, 35] This provides information about the majority carrier type, intermediate states, and the effective band gap of the semiconductor, with high sensitivity.[29, 34-36] We chose n-$BiVO_4$ for this study because it is a known photoanode [37-43] and photocatalyst material for water oxidation under 2.5 eV bandgap illumination. [23, 43-45] As second absorber, p-Cu_2O (2.1 eV) is used because it is a promising photocathode material for tandem PEC devices. [46;47] As we show in the following, a tandem junction is formed at the $BiVO_4$-Cu_2O interface by simply layering these nanoparticles and by mildly annealing at 350 ^{0}C. This suggest the possibility of artificial photosynthetic system based on powders of these two materials. It may also explain the improved photocatalytic dye degradation performance of Cu_2O/$BiVO_4$ composites previously reported in the literature. [48-50] Cu_2O nanoparticles for the study were synthesized from copper(II) acetylacetonate in acetone (Details in Supporting Information). [51] The reaction affords Cu_2O nanoparticles in the Cuprite structure type with an average size of 59 ± 17 nm (**Figure 1E,** XRD in **Figure S1**) and cubic microcrystals, with 1 µm edge length (**Figure 1F**). Based on TEM images, the mass ratio of both particle sizes is 1:1. The $BiVO_4$ nanoparticles for the study were synthesized from Bi_2O_3 and V_2O_5 in acetic acid, using a revised method.[49] The material crystallizes in the Scheelite structure

Department of Chemistry, University of California, Davis. One Shields Avenue, Davis, CA, 95616, USA. Fax: (+1)530 752 8995; E-mail: fosterloh@ucdavis.edu

† Electronic Supplementary Information (ESI) available: Experimental Details, XRD, SEM and UV/vis data. DOI: 10.1039/x0xx00000x

This journal is © The Royal Society of Chemistry 20xx

Please do not adjust margins

type (**Figure S1**) and forms particles of 73 ± 35 nm average size (**Figure 1B**).

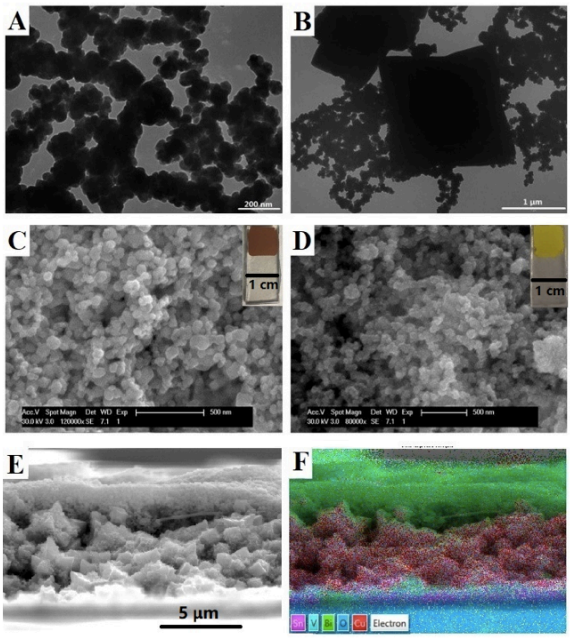

Figure 1. Transmission electron microscope images for A) $BiVO_4$ and B) for Cu_2O particles. Scanning electron microscope images for C) Cu_2O single layer, top view (photo in insert) and D) $BiVO_4$ single layer, top view (photo in insert). E) FTO-$BiVO_4$-Cu_2O double layer, cross view. F) Energy-dispersive X-ray spectroscopy (EDS) element map overlaid onto SEM image.

Thin films of the particles were prepared by drop-casting suspensions on FTO substrates, followed by drying in air and annealing at 350°C under argon for 5h. These films have a red-brown (Cu_2O) or yellow ($BiVO_4$) appearance and contain the particles in loosely packed form (**Figure 1CD** and inserts). Surface photovoltage and optical spectra for separate $BiVO_4$ and Cu_2O particle films on FTO are presented in **Figure 2**. The spectrum for $BiVO_4$ contains a negative photovoltage feature that can be attributed to photoinduced electron transport to the FTO substrate, as expected for an n-type semiconductor.[52] The 2.45 eV onset is slightly below the 2.55 eV optical absorption onset of the material (**Figure 2**), which is attributed to defect states near the band edges. In contrast, the photovoltage signal for the Cu_2O particle film on FTO has a positive sign. Here, the voltage results from injection of *hole* majority carriers into the FTO substrate. The onset energy of 2.0 eV corresponds well to the absorption spectrum of the material and to the optical band gap reported in the literature. [56] The photovoltage spectra can be understood on the basis of the energetics of the FTO/sample configurations, as shown in **Figure 3A** and **B**. Fundamentally, the photovoltage of a particle film is determined by the offset of the FTO workfunction (Fermi energy) and the band edges of the light absorber. These offsets are +0.3 V and -0.35 V for Cu_2O and $BiVO_4$ on FTO, respectively. The experimentally observed photovoltage values (+70 mV for Cu_2O and -165 mV for $BiVO_4$) are substantially lower, which is attributed mainly to the low light intensity of the light source (0.1 to 0.3 mW cm^{-2}). For example, in a previous study it was found that the photovoltage was found to vary with the logarithm of the light intensity. [34, 53] Another reason is that the sample film thickness is below the optical absorption depth of each material (see discussion below).

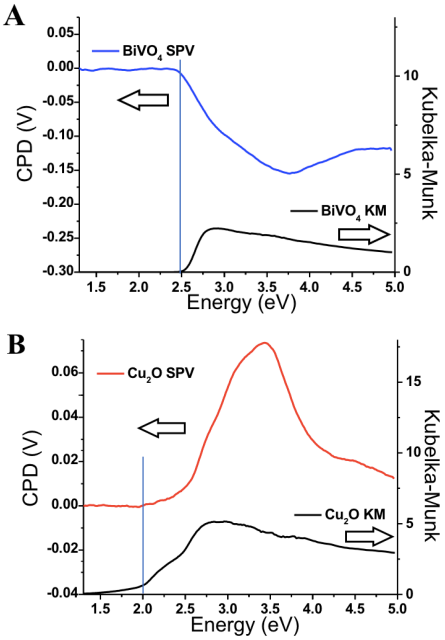

Figure 2. Surface photovoltage spectra and diffuse reflectance optical absorption spectra of A) 0.80 micrometer thick $BiVO_4$ film on fluorine doped tin oxide (FTO), and B) 0.72 micrometer thick Cu_2O film on FTO. KM stands for Kubelka-Munk.

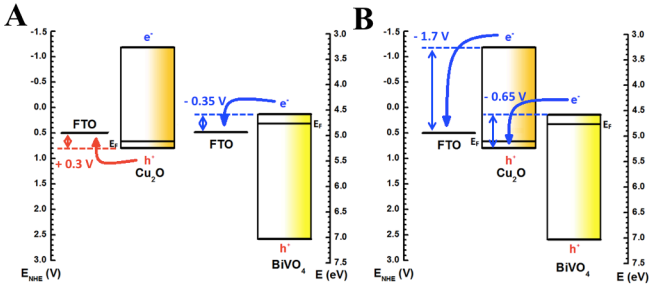

Figure 3. Energy scheme for A) FTO/Cu_2O and FTO/$BiVO_4$ single layer films and B) energy scheme for FTO/Cu_2O/$BiVO_4$ bilayer film using band edges from the literature. [44, 46]

Next, to evaluate photochemical charge transfer between Cu_2O and $BiVO_4$, a stacked particle film was assembled by two sequential drop-casting steps each followed by annealing in argon at 350 °C. Scanning electron micrographs of the stacked film are shown in **Figure 1C/D** together with EDS analysis results in **Figures 1D** and **S2.** Two distinct 3-5 micrometer thick layers of $BiVO_4$ nanoparticles at the top and loosely packed Cu_2O nano- and microparticles at the bottom can be observed. Elemental mapping confirms the composition of each layer with no particle intermixing occurring. Surface photovoltage spectra for FTO/Cu_2O/$BiVO_4$ stacks with variable layer thicknesses are shown in **Figure 4**. Layer thicknesses were chosen in the 2.5 to 5 µm range to ensure optimal light absorption and charge transport. In all cases, a strongly negative photovoltage is observed above 2.25 eV. This voltage reaches a maximum

This journal is © The Royal Society of Chemistry 20xx

around 2.5 eV where both materials can absorb light (**Figure 4A**), and then decays at higher photon energies, due to the decrease in light penetration depth at higher photon energy. The sign of the voltage and its size indicates that both absorbers now act in tandem, as shown in the excitation scheme in **Figure 3B**. Holes from Cu_2O are no longer injected into the bottom FTO but into the top $BiVO_4$ layer where they recombine with majority carriers formed under $BiVO_4$ excitation. This reversal of the charge transfer direction in the Cu_2O particle layer is attributed to the Ohmic nature of the Cu_2O-$BiVO_4$ contact, which promotes majority carrier transfer across this interface.

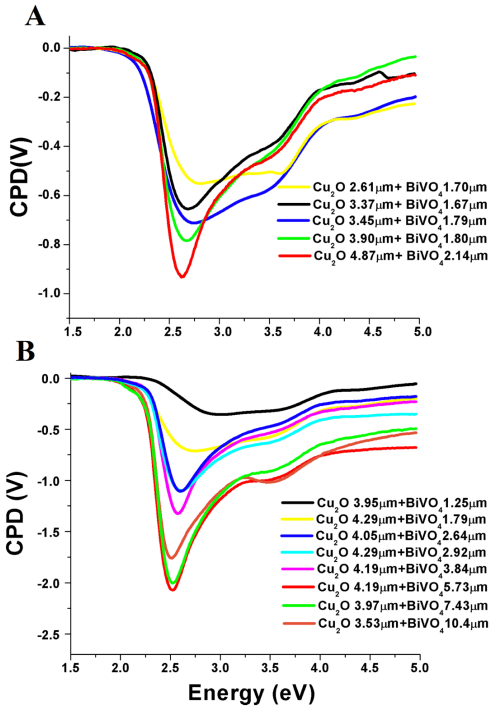

Figure 4. Surface photovoltage spectra for FTO-Cu_2O-$BiVO_4$ bilayer stacks. A) with variable Cu_2O layer thickness and nearly constant $BiVO_4$ layer thickness, B) with variable $BiVO_4$ layer thickness and nearly constant Cu_2O layer thickness.

As can be seen from **Figure 4**, the shape of the photovoltage spectra and the maximum photovoltage depend strongly on the thickness of the Cu_2O and $BiVO_4$ layers. Spectra in **Figure 4A** were acquired for variable Cu_2O layer thickness while holding the $BiVO_4$ layer constant at ~2 micrometer. As the Cu_2O particle layer gets thicker, the photovoltage maximum increases and reaches -0.93 V for a 4.8 μm thick film. This linear dependence (see also plot in **Figure 5A**) is expected if the photovoltage is limited by the light harvesting ability of the Cu_2O layer. The optical absorption coefficient for Cu_2O single crystals is 7.0×10^5 cm^{-1} at 2.5 eV, [54] which corresponds to an optical penetration depth of $1/\alpha$= 1.43 μm (or $3/\alpha$=4.3 μm to absorb 95% of the incoming light). For loosely packed Cu_2O particles, $3/\alpha$ will be greater, which confirms that light harvesting is a limiting issue in the particle layer. Incomplete light absorption at 2.5 eV is the likely reason why the photovoltage maximum for the thinnest Cu_2O film (2.61 μm) occurs at 2.8 eV, where light absorption is improved. Some of this effect is seen for the 3.45 μm thick film, which is attributed to thickness variations across the 1.0 cm^2 sample. **Figure 4B** summarizes spectra acquired for FTO/Cu_2O/$BiVO_4$ stacks with the Cu_2O layer held constant at ~4 μm and **Figure 5** plots the maximum photovoltage versus $BiVO_4$ layer thickness. It can be seen that the photovoltage increases until the $BiVO_4$ layer thickness reaches 5.73 μm and then decreases for thicker films. This behaviour was previously observed for a silicon-$BiVO_4$ tandem.[52] It was attributed to limiting light absorption in the thin films and limiting charge transport in the thicker films. A balance between these two parameters occurs at 5.73 μm. This value is below light penetration depth ($3/\alpha$=9.1 μm for 95% light absorption) of a $BiVO_4$ particle film (**Figure S3**).

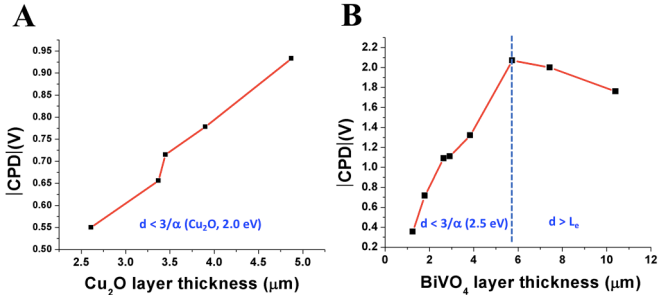

Figure 5. Photovoltage versus A) Cu_2O thickness and versus B) $BiVO_4$ thickness d. L_e : electron diffusion length, α : optical absorption coefficient at 2.5 eV.

That indicates that electron diffusion in $BiVO_4$ is limiting the photovoltage. Indeed, for non-doped $BiVO_4$, the electron diffusion length, L_e, is only 10-70 nm. [55, 56] The SPS data in **Figure 4B** also shows a shift of the photovoltage maximum position to lower photon energy as the $BiVO_4$ layer thickness increases. This is because the light passing through the $BiVO_4$ film becomes increasingly red shifted. An optimized FTO/Cu_2O/$BiVO_4$ stack at 4.19 μm Cu_2O and 5.73 μm $BiVO_4$ generates the largest photovoltage of -2.1 V at 2.5 eV. This photovoltage corresponds to 90% of the theoretically possible voltage (-2.35 V), as defined by sum of the E_{CB}-E_F offsets at the Cu_2O –FTO interface (-1.7 V) and the E_{VB}-E_{CB} offset at the Cu_2O-$BiVO_4$ interface (-0.65 V) in **Figure 3B**. Based on this analysis, photochemical charge separation in the FTO/Cu_2O/$BiVO_4$ stack is 90% efficient under the vacuum conditions of the SPS experiment.

In conclusion, we have employed surface photovoltage spectroscopy to observe photochemical charge transfer in Cu_2O and $BiVO_4$ particle films as a function of wavelength for the first time. Isolated Cu_2O particle layers on FTO show p-type behavior and $BiVO_4$ particles show n-type behavior. In a FTO/Cu_2O/$BiVO_4$ particle stack, both particles act in tandem, producing up to -2.1 V photovoltage under 2.5 eV excitation, which corresponds to 90% of the ideal limit. The photovoltage spectra also reveal the effects of shading at high excitation energy and the effects of low absorber strength at low excitation energy. These results are relevant to the understanding of photochemical charge transfer at irregular particle surfaces and to the construction of devices for artificial photosynthesis and water splitting.

This work was supported through funding from the U.S. Department of Energy, Office of Science, Office of Basic Energy Sciences under Award Number DE-SC0015329.

Notes and references

1. M. G. Walter, E. L. Warren, J. R. McKone, S. W. Boettcher, Q. X. Mi, E. A. Santori and N. S. Lewis, *Chem. Rev.*, 2010, **110**, 6446-6473.

2. M. S. Prévot and K. Sivula, *J. Phys. Chem. C*, 2013, **117**, 17879-17893.
3. J. R. Bolton, S. J. Strickler and J. S. Connolly, *Nature*, 1985, **316**, 495-500.
4. O. K. Varghese and C. A. Grimes, *Sol. Energ. Mat. Sol. C*, 2008, **92**, 374-384.
5. S. Hu, C. X. Xiang, S. Haussener, A. D. Berger and N. S. Lewis, *Energ. & Environ. Sci.*, 2013, **6**, 2984-2993.
6. L. C. Seitz, Z. Chen, A. J. Forman, B. A. Pinaud, J. D. Benck and T. F. Jaramillo, *ChemSusChem*, 2014, **7**, 1372-1385.
7. M. C. Hanna and A. J. Nozik, *J. Appl. Phys.*, 2006, **100**.
8. R. E. Rocheleau and E. L. Miller, *Int. J. Hydrogen Energ.*, 1997, **22**, 771-782.
9. K. T. Fountaine, H. J. Lewerenz and H. A. Atwater, *Nat. Commun.*, 2016, **7**, 13706.
10. S. Licht, B. Wang, S. Mukerji, T. Soga, M. Umeno and H. Tributsch, *Int. J. Hydrogen Energ.*, 2001, **26**, 653-659.
11. A. E. Delahoy, S. C. Gau, O. J. Murphy, M. Kapur and J. O. M. Bockris, *Int. J. Hydrogen Energ.*, 1985, **10**, 113-116.
12. C. Gramaccioni, A. Selvaggi and F. Galluzzi, *Electrochim. Acta*, 1993, **38**, 111-113.
13. G. H. Lin, M. Kapur, R. C. Kainthla and J. O. M. Bockris, *Appl. Phys. Lett.*, 1989, **55**, 386-387.
14. S. Y. Reece, J. A. Hamel, K. Sung, T. D. Jarvi, A. J. Esswein, J. J. H. Pijpers and D. G. Nocera, *Science*, 2011, **334**, 645-648.
15. O. Khaselev and J. A. Turner, *Science*, 1998, **280**, 425-427.
16. E. Verlage, S. Hu, R. Liu, R. J. R. Jones, K. Sun, C. Xiang, N. S. Lewis and H. A. Atwater, *Energ. & Environ. Sci.*, 2015, **8**, 3166-3172.
17. M. R. Shaner, K. T. Fountaine, S. Ardo, R. H. Coridan, H. A. Atwater and N. S. Lewis, *Energ. Environ. Sci.*, 2014, **7**, 779-790.
18. R. H. Coridan, K. A. Arpin, B. S. Brunschwig, P. V. Braun and N. S. Lewis, *Nano Lett.*, 2014, **14**, 2310-2317.
19. M. G. Kibria, H. P. T. Nguyen, K. Cui, S. Zhao, D. Liu, H. Guo, M. L. Trudeau, S. Paradis, A.-R. Hakima and Z. Mi, *ACS Nano*, 2013, **7**, 7886-7893.
20. B. Fujihara, T. Ohno and M. Matsumura, *J. Chem. Soc., Faraday T.*, 1998, **94**, 3705-3709.
21. H. Kato, M. Hori, R. Konta, Y. Shimodaira and A. Kudo, *Chem. Lett.*, 2004, **33**, 1348-1349.
22. Q. Jia, A. Iwase and A. Kudo, *Chem. Sci.*, 2014, **5**, 1513-1519.
23. R. Abe, K. Sayama and H. Sugihara, *J. Phys. Chem. B*, 2005, **109**, 16052-16061.
24. K. Maeda, M. Higashi, D. L. Lu, R. Abe and K. Domen, *J. Am. Chem. Soc.*, 2010, **132**, 5858-5868.
25. M. Higashi, R. Abe, K. Teramura, T. Takata, B. Ohtani and K. Domen, *Chem. Phys. Lett.*, 2008, **452**, 120-123.
26. M. Higashi, R. Abe, A. Ishikawa, T. Takata, B. Ohtani and K. Domen, *Chem. Lett.*, 2008, **37**, 138-139.
27. K. Domen, A. Kudo and T. Onishi, *J. Catal.*, 1986, **102**, 92-98.
28. R. L. Chamousis and F. E. Osterloh, *Energ. & Envi. Sci.*, 2014, **7**, 736-743.
29. J. Wang, J. Zhao and F. E. Osterloh, *Energ. & Envi. Sci.*, 2015, **8**, 2970-2976.
30. H. C. Gatos and J. Lagowski, *J. Vac. Sci. Technol.*, 1973, **10**, 130-135.
31. L. Kronik and Y. Shapira, *Surf. Interface Anal.*, 2001, **31**, 954-965.
32. D. Heredia, L. Otero, M. Gervaldo, F. Fungo, T. Dittrich, C.-Y. Lin, L.-C. Chi, F.-C. Fang and K.-T. Wong, *Thin Solid Films*, 2013, **527**, 175-178.
33. T. Dittrich, A. Gonzáles, T. Rada, T. Rissom, E. Zillner, S. Sadewasser and M. Lux-Steiner, *Thin Solid Films*, 2013, **535**, 357-361.
34. M. A. Melo, Z. Wu, B. A. Nail, A. T. De Denko, A. F. Nogueira and F. E. Osterloh, *Nano Lett.*, 2018, **18**, 805-810.
35. J. Zhao, B. A. Nail, M. A. Holmes and F. E. Osterloh, *J. Phys. Chem. Lett.*, 2016, DOI: 10.1021/acs.jpclett.6b01569, 3335-3340.
36. X. Ma, X. Cui, Z. Zhao, M. A. Melo, E. J. Roberts and F. E. Osterloh, *Journal of Materials Chemistry A*, 2018, **6**, 5774-5781.
37. J. A. Seabold and K. S. Choi, *J. Am. Chem. Soc.*, 2012, **134**, 2186-2192.
38. Y. Q. Liang, T. Tsubota, L. P. A. Mooij and R. van de Krol, *J. Phys. Chem. C*, 2011, **115**, 17594-17598.
39. S. P. Berglund, D. W. Flaherty, N. T. Hahn, A. J. Bard and C. B. Mullins, *J. Phys. Chem. C*, 2011, **115**, 3794-3802.
40. S. J. Hong, S. Lee, J. S. Jang and J. S. Lee, *Energ. & Environ. Sci.*, 2011, **4**, 1781-1787.
41. S. K. Pilli, T. E. Furtak, L. D. Brown, T. G. Deutsch, J. A. Turner and A. M. Herring, *Energ. & Environ. Sci.*, 2011, **4**, 5028-5034.
42. D. K. Zhong, S. Choi and D. R. Gamelin, *J. Am. Chem. Soc.*, 2011, **133**, 18370-18377.
43. A. Kudo, K. Ueda, H. Kato and I. Mikami, *Catal. Lett.*, 1998, **53**, 229-230.
44. J. Wang and F. E. Osterloh, *J. Mater. Chem. A*, 2014, **2**, 9405-9411.
45. R. G. Li, F. X. Zhang, D. G. Wang, J. X. Yang, M. R. Li, J. Zhu, X. Zhou, H. X. Han and C. Li, *Nat Commun*, 2013, **4**.
46. A. Paracchino, N. Mathews, T. Hisatomi, M. Stefik, S. D. Tilley and M. Gratzel, *Energ. & Environ. Sci.*, 2012, **5**, 8673-8681.
47. P. Bornoz, F. F. Abdi, S. D. Tilley, B. Dam, R. van de Krol, M. Graetzel and K. Sivula, *J. Phys. Chem. C*, 2014, **118**, 16959-16966.
48. H. Li, W. Hong, Y. Cui, X. Hu, S. Fan and L. Zhu, *Materials Science and Engineering: B*, 2014, **181**, 1-8.
49. W. Wang, X. Huang, S. Wu, Y. Zhou, L. Wang, H. Shi, Y. Liang and B. Zou, *Applied Catalysis B: Environmental*, 2013, **134-135**, 293-301.
50. E. Aguilera-Ruiz, U. M. García-Pérez, M. de la Garza-Galván, P. Zambrano-Robledo, B. Bermúdez-Reyes and J. Peral, *Appl. Surf. Sci.*, 2015, **328**, 361-367.
51. A. Singhal, M. R. Pai, R. Rao, K. T. Pillai, I. Lieberwirth and A. K. Tyagi, *Eur J Inorg Chem*, 2013, DOI: DOI 10.1002/ejic.201201382, 2640-2651.
52. Y. Yang, J. Wang, J. Zhao, B. A. Nail, X. Yuan, Y. Guo and F. E. Osterloh, *ACS Appl. Mater. & Interfaces*, 2015, **10**, 5959–5964.
53. J. Zhao and F. E. Osterloh, *J. Phys. Chem. Lett*, 2014, **5**, 782–786.
54. T. Ito, T. Kawashima, H. Yamaguchi, T. Masumi and S. Adachi, *J. Phys. Soc. Jpn.*, 1998, **67**, 2125-2131.
55. J. A. Seabold, K. Zhu and N. R. Neale, *Phys. Chem. Chem. Phys.*, 2014, **16**, 1121-1131.
56. F. F. Abdi, T. J. Savenije, M. M. May, B. Dam and R. van de Krol, *J. Phys. Chem. Lett.*, 2013, **4**, 2752-2757.

This journal is © The Royal Society of Chemistry 20xx

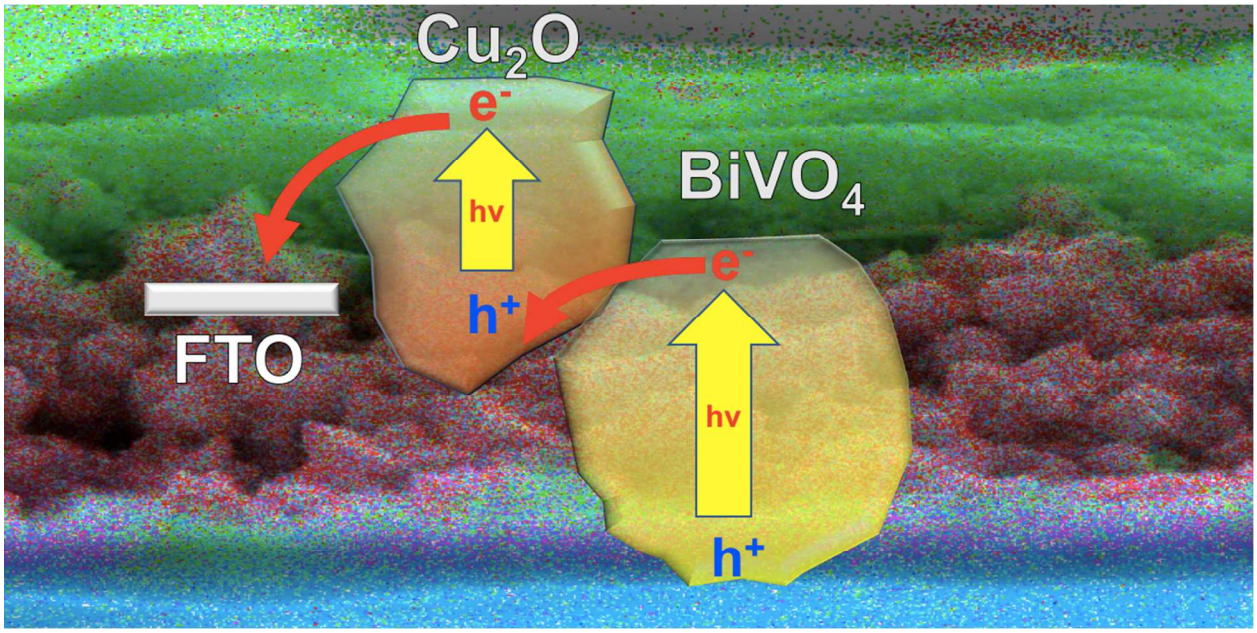

Surface photovoltage spectroscopy resolves wavelength-dependent photochemical charge transfer between irregularly shaped $BiVO_4$ and Cu_2O particles for the first time.